On Promoting Intercalation and Exfoliation of Bentonite in High-Density Polyethylene by Grafting Acrylic Acid

Yuzhen Xu, Zhengping Fang, Lifang Tong

Institute of Polymer Composites, Zhejiang University, Hangzhou 310027, China

ABSTRACT: Acrylic acid (AA) grafted high-density polyethylene (HDPE)/bentonite (BT) composites and HDPE/BT composites were prepared via melt compounding. XRD and TEM results indicated that the modification of AA grafting promoted the dispersion and intercalation of BT in HDPE matrix; IR proved that there were interactions between AA and BT sheets. Consequently, with increasing BT content, the tensile strength and Young's modulus of HDPE-*g*-AA/BT nanocomposites increased, while that of HDPE/BT composites decreased. Moreover, the addition of BT to HDPE-*g*-AA decreased the ability of crystallization of the matrix. © 2005 Wiley Periodicals, Inc. J Appl Polym Sci 96: 2429–2434, 2005

Key words: acrylic acid; graft copolymers polyethylene; bentonite; nanocomposites

INTRODUCTION

Intercalation of polymer melts in layered silicates of synthetically modified clay such as lipophilized bentonite has recently become better understood as a good tool to prepare composite material exhibiting excellent thermal, gas barrier, and mechanical properties.[1–8] The enhanced properties of nanocomposites have attracted extensive research interest in polymer/clay nanocomposites in recent years.[9]

Polyethylene is one of the most widely used polyolefins. Since it does not include any polar group in its backbone, the homogeneous dispersion and exfoliation of the clay minerals in polyethylene is not realized even when the clay is organically modified.[10–12] Gopakumar[13] also considered that, if we want to prepare PE/clay nanocomposites, two conditions are required to produce the intensity of surface interactions required to exfoliate and disperse the clay in polyethylene: First, the bentonite clay must be ion-exchanged to reduce the cohesive forces between clay platelets; second, the PE must be chemically modified to improve adhesion between the PE and clay filler. So it is necessary to induce polar groups in PE chains so as to mediate the polarity between clay and PE matrix. Chemical modification of polyethylene had been used successfully to overcome problems associated with poor dispersion and interfacial adhesion in a polyethylene/clay system. One of the typical examples is the polyethylene/silicate nanocomposite system suggested by Wang et al.[14,15] They prepared maleic anhydride (MA) grafting LDPE and organophilic clay nanocomposites by melt compounding. On the one hand, the hydrophobicity of the organically modified bentonite increases as the carbon number of organic modifier increases. On the other hand, the hydrophilicity of polyethylene increases as the grafting level of MA in polyethylene. This result suggests that, to obtain good dispersion of clay in matrix, the polyethylene should have a certain grafting level of MA in matrix.

Acrylic acid(AA) as well as maleic anhydride is a good polar monomer. It has been widely used to graft polyethylene to induce polar groups in PE chains. Furthermore the carboxyl of AA can react with the hydroxy of BT, so it is better than other modifiers. However, AA grafing HDPE is more difficult than AA grafting LDPE because HDPE has structural regularity, and it is difficult to produce active sites. Research efforts have been extensively devoted to the development of novel synthetic approaches as well as to the investigation of the physical properties in LDPE nanocomposites: it is necessary to investigate the preparation of chemically modified HDPE nanocomposites.

In this work, first we prepared HDPE-*g*-AA composites that have both high grafting degree and high grafting efficiency. Second we present the fine structure and morphology of the intercalated HDPE-*g*-AA having different BT contents and prove that reactions between the carboxyl of AA and the hydroxy of BT exist. Finally, mechanical properties and thermal properties of HDPE-*g*-AA/BT composites were investigated and compared with the HDPE/BT system.

Correspondence to: Z. Fang (zpfang@zju.edu.cn).
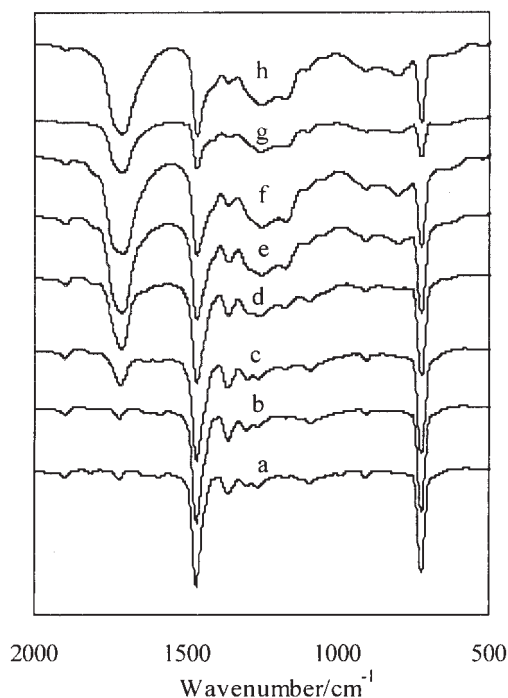
Figure 1 FT-IR spectra of HDPE and HDPE-*g*-AA: (a) pure HDPE, (b–h) HDPE/AA/DCP (100/*x*/0.2): AA contents; (b) 0 phr, (c) 1 phr, (d) 2 phr, (e) 5 phr, (f) 10 phr, (g) 20 phr, (h) 40 phr.

EXPERIMENTAL

Materials

The organically modified bentonite (C18-BT) was supplied by Zhejiang Huate Clay Products of China and was ion-exchanged with octadyl trimethyl ammonium. High-density polyethylene (5502#, MFR = 0.35 g/10 min) was from Daelim Corp., Korea. Acrylic acid and dicumyl peroxide (DCP) were used as the grafting monomer and a radical initiator of high-density polyethylene, respectively. All chemicals were used without further purification.

Preparation of composites

All composites were prepared via melt compounding at 160°C in a ThermoHaake Rheomix with a screw speed of 60 rpm, and the mixing time was 20 min for each sample. The mixed samples were transferred to a

TABLE I
The Elemental Analysis Results of HDPE/AA/DCP
(100/*x*/0.2, mass ratio)

| AA content (phr)	1	2	5	10	20	40
Content of oxygen (%)	0.40	0.83	1.81	3.73	4.26	5.64
Grafting degree (%)	0.90	1.86	4.07	8.39	9.57	12.68
Grafting efficiency (%)	90	93	81	84	48	32
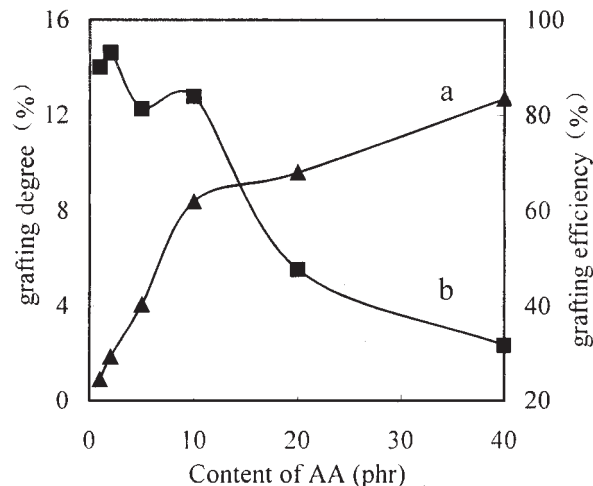
Figure 2 The relationship between the content of AA and the grafting degree and grafting efficiency of HDPE/AA/DCP (100/*x*/0.2): (a) grafting degree; (b) grafting efficiency.

mold and preheated at 160°C for 3 min and then pressed at 14 MPa and successively cooled to room temperature while maintaining the pressure to obtain the composite sheets for further measurements.

Characterization

FT-IR spectra

The FT-IR spectra were recorded on a Vector-22 FT-IR spectrometer. The samples were dissolved in xylene at
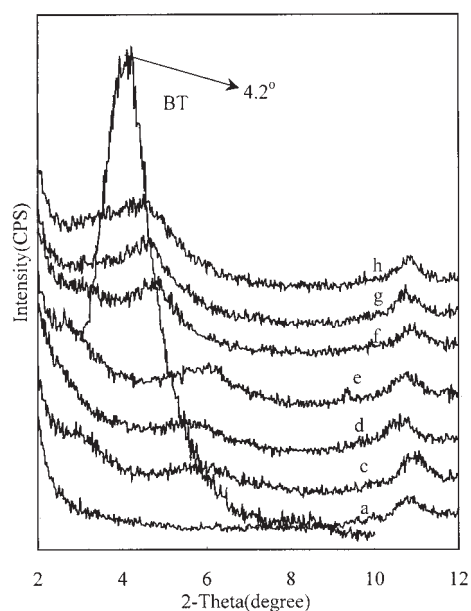
Figure 3 XRD patterns of BT, HDPE/BT, and HDPE-*g*-AA/BT: (a) pure HDPE, (c–e) HDPE-*g*-AA/BT (2, 3, and 4 phr, respectively); (f–h) HDPE/BT (2, 3, and 4 phr, respectively).
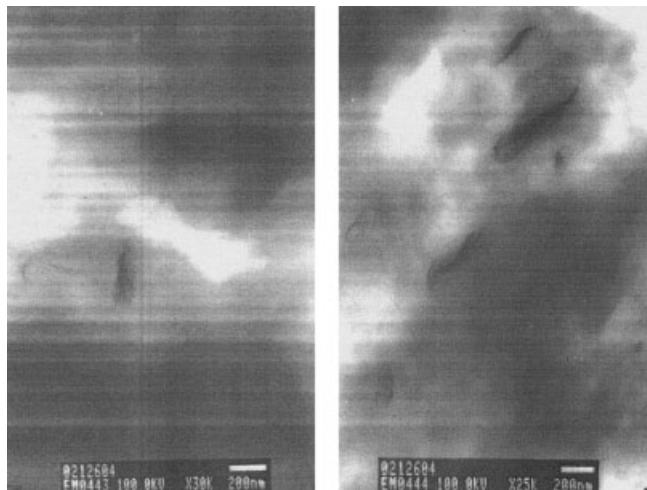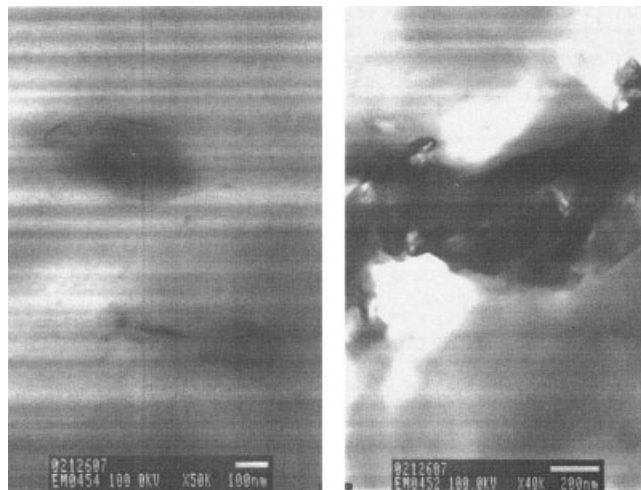
Figure 4 TEM observations for HDPE-g-AA/2 phr BT.

a concentration of 2 wt % and were precipitated by alcohol and then filtered and dried in a vacuum oven at 80°C for 24 h. Finally, the purified samples were pressed to obtain membranes whose thicknesses were about 40 ~ 60 μm.

Elemental analysis

Elemental analyis was performed in a Parloerba EA1110 Elemental Analyzer. The samples were treated with the same method as in the FT-IR measurements. The contents of carbon, hydrogen, and oxygen were measured, and the grafting degree (P) and grafting efficiency (E) could be calculated according to the following equations:

$$P = \frac{M_1}{2M_2} \times w_O \qquad (1)$$

$$E = \frac{P}{w_{AA}} \qquad (2)$$

Where M_1 is the molecular weight of the AA monomer; M_2 is the molar weight of the oxygen atom; w_o is the weight percentage of oxygen; and w_{AA} is the percentage of AA.

X-ray diffraction

X-ray diffraction (XRD) was used to examine the dispersion of BT in composites. XRD was carried out by using a Rigaku X-ray generator (Cu Kα radiation with λ = 1.54 Å) at room temperature. The diffractograms were obtained at the scattering angles from 2 to 12°, at a scanning rate of 4°/min.
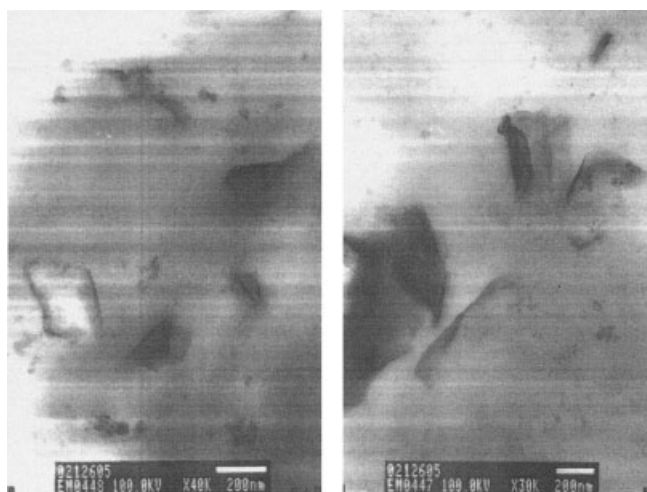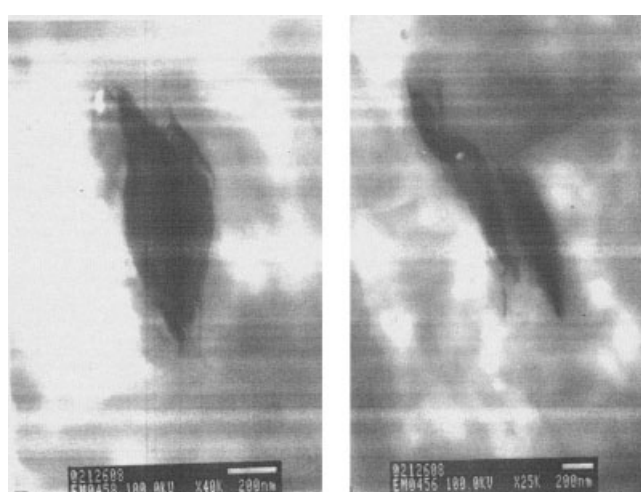

Figure 6 TEM observations for HDPE/2 phr BT.

Figure 5 TEM observations for HDPE-g-AA/3 phr BT.

Figure 7 TEM observations for HDPE/3 phr BT.

TABLE II
Extraction Data of HDPE, HDPE-*g*-AA, and Their Composites with BT

	HDPE	HDPE-*g*-AA	HDPE/4 phr BT	HDPE-*g*-AA/4 phr BT
Theoretical extraction rate(%)	100	90.9	96.2	89.3
Actual extraction rate(%)	100	80.7	96.3	82.4

Transmission electron microscopy

The transmission electron micrographs were obtained with a JEM-1200EX electron microscope to examine the dispersion and exfoliation status of BT in composites. The nanocomposite samples for TEM observation were ultrathin-sectioned using a microtome equipped with a diamond knife. The sections ($100 \sim 200$ nm) were cut from a piece of about 1×1 mm^2, and they were collected in a trough filled with water and placed on 200 mesh copper grid.

Differential scanning calorimetry

Thermal properties of composites were measured with a Perkin–Elmer 7 Differential Scanning Calorimeter (DSC). Samples were heated from 40 to 180°C at a rate of 10°C/min under a nitrogen atmosphere.

Mechanical testing

Mechanical properties of composite were measured using an RG2000–10 Universal Tensile Tester according to ASTM D 638 standard. Five samples of each batch were measured. The samples were performed

Figure 8 FT-IR spectra of cure BT and the drawers of HDPE-*g*-AA/3 phr BT and HDPE/3 phr BT: (a) cure BT; (b) the drawer of HDPE-*g*-AA/3 phr BT; (c) the drawer of HDPE/3 phr BT.

with a 50 mm/min extension rate at room temperature.

Extraction and characterization

Extraction of polyethylene chain from the PE-*g*-AA/BT and PE/BT composites was carried out using hot solvent (xylene) in a Soxhlet extractor at 140°C for 48 h and then filtered and dried in a vacuum oven at 80°C for 10 h. Whereafter these samples were extracted again by alcohol at 80°C for 24 h to extract the homopolymer of polyacrylic acid, and then filtered and dried in a vacuum oven at 60°C. Finally, these samples were characterized by FT-IR.

RESULTS AND DISCUSSION

Preparation of AA grafted HDPE by melt compounding

HDPE-*g*-AA was prepared by melt grafting. To measure the content of AA grafted on HDPE, the samples obtained after reaction were predried to remove the unreacted AA monomers in a vacuum oven at 60°C for 5 h. The dried samples were dissolved in xylene at a concentration of 2 wt %. This solution was mixed with alcohol and the precipitate was filtered and dried again in a vacuum oven at 80°C for 24 h. The percentage of AA grafted on HDPE was determined by elemental analysis and FT-IR spectra.

Figure 1 shows the FT-IR spectra of HDPE and HDPE-*g*-AA. It is found that new peaks appear at 1710 cm^{-1} (carbonyl group) compared to the pure HDPE, indicating that AA has been successfully grafted onto the polyethylene chain. Moreover, with increasing the content of AA, the height of the peak at 1710 cm^{-1} increased, consistent with the increment of AA weight percentage.

The result was affirmed by elemental analysis (Table I and Fig. 2). When AA content was less than 10 phr (g/100 g HDPE), the grafting degree increased remarkably with increasing the content of AA loaded, and the grafting efficiency was maintained at a level greater than 80%. However, when AA content exceeded 10 phr, the increment of the extent of grafting level off and the grafting efficiency decreased remarkably. This is due to a competition between the graft copolymerization and the self-polymerization of AA in the system. When the loading content of AA was
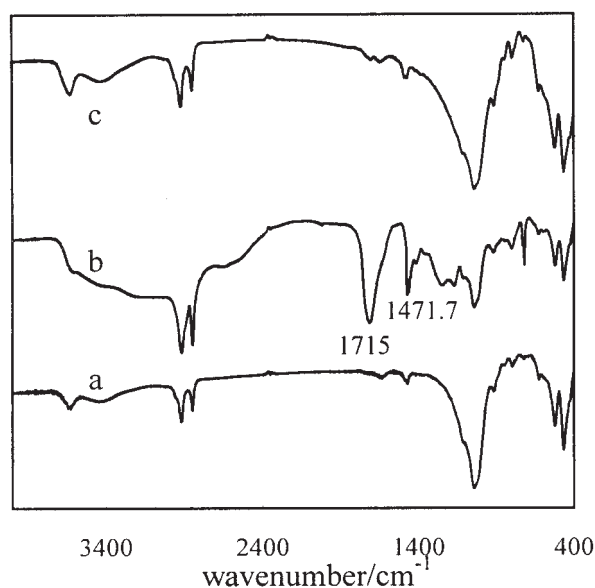
TABLE III
Mechanical and Thermal Properties of HDPE, HDPE-g-AA, and Their Composites with BT

Samples	HDPE/BT				HDPE-g-AA[a]/BT			
BT content (phr)	0	2	3	4	0	2	3	4
Tensile strength (MPa)	32.5	32.9	32.1	31.9	32.7	34.2	33.5	35.0
Elongation at break (%)	144.1	66.1	58.9	52.0	35.1	22.6	25.0	31.2
Young's modulus (MPa)	366.7	367.1	352.8	329.5	425.1	434.4	464.4	485.2
Melting temperature (°C)	133.5	133.5	133.7	134.2	132.8	132.4	132.5	132.1
Melting endotherms (J/g)	205.3	208.0	205.6	206.5	205.8	195.2	193.8	194.2

[a] HDPE-g-AA: 100 g HDPE grafted with 10 g AA initiated by 0.2 g DCP.

high enough, AA could easily polymerize itself, owing to its higher reactivity than polyethylene. In comparison, when the content of AA is low, the possibility that AA radicals attack PE chains would be much higher than other AA monomers. Thus, the principle reaction should be graft copolymerization and grafting efficiency maintained at a high level. In the following experiments, we selected 10 phr AA grafting HDPE, which has both a high grafting degree and a high grafting efficiency, to prepare the nanocomposites with BT.

The dispersion of C18-BT in HDPE and HDPE-g-AA

The direct evidence of the intercalation is provided by the XRD patterns of the obtained hybrids. The (001) plane peak of BT was around $2\theta = 4.2$. The XRD pattern of the mixture of C18-BT (2 phr, 3 phr, 4 phr) with HDPE is presented in Figure 3. The result clearly shows that the (001) plane peak of the clay does not change and polyethylene chains do not intercalate into BT. It is because polyethylene does not include any polar group in its backbone, and the silicate layer of clay, even modified by nonpolar long alkyl groups, is polar and incompatible with polyolefin.

Figure 3 also shows the XRD patterns of HDPE-g-AA compounding with the same content of BT. Compared to these curves the (001) plane peak at $2\theta = 4.2$ disappeared, revealing the exfoliation of BT. This result indicates that the modification of AA grafting mediates the polarity between PE and BT and promotes the penetration of PE chains into layered BT. In curves c–e, we can find a weak peak at $2\theta = 5 \sim 7°$. From our point of view, this peak might be correspond to the (002) plane of BT, which showed a shoulder at $2\theta = 8 \sim 9°$.

To confirm the dispersion of BT in HDPE-g-AA and pure HDPE, TEM was used to directly view the structure of nanocomposites (Figs. 4, 5, 6, and 7). Obviously, the dispersion of BT was much better in the HDPE-g-AA/BT composites (Figs. 4 and 5) than in HDPE/BT composites (Figs. 6 and Fig. 7). Some of the BT has exfoliated into single sheets in HDPE-g-AA/BT composites. While in HDPE/BT composites, BT aggre-gates are not intercalated by PE chains. It is realized that polyethylene nanocomposite with good exfoliation or intercalation can be obtained by proper modification of HDPE.

The reaction between PE-g-AA and BT

The dispersion of BT in PE-g-AA is better than in pure PE, not only because of the increasing of polarity of PE, but also because of the reaction between HDPE-g-AA and BT, which was ion-exchanged with octadyl trimethyl ammonium. The HDPE-g-AA chain has carboxyl groups that can react with the amino groups. This suggestion can be confirmed by the extraction result (Table II) and FT-IR spectra (Fig. 8). Results in Table II show that polyethylene has been totally extracted in pure HDPE and HDPE/BT, while in HDPE-g-AA/BT part of the HDPE could not be extracted. Comparing curve (a) with (c) in Figure 8, we can see that the two curves are completely the same, revealing that all of the HDPE has been extracted. While in curve (b), there is the characteristic peak of acrylic acid at 1715 cm^{-1} and the characteristic peak of polyethylene at 1471.7 cm^{-1}. These results indicated that there might be a chemical bond between BT and HDPE-g-AA, and it improved the intercalation and exfoliation of BT in matrix.

Mechanical properties

Table III lists the tensile strength, elongation at break, and Young's modulus for HDPE-g-AA and their BT composites. When adding 2, 3, and 4 phr BT to HDPE-g-AA, respectively, it is found that the tensile strength and modulus both increased with increments of BT content, while the elongation at break was maintained at a low level.

In comparison, when adding the same content of BT to HDPE, we found that all mechanical properties decreased. It is because BT cannot disperse well in HDPE matrix or sometimes gathers, that leads to cavities in the matrix.

As we know, the mechanical properties of the composites are strongly related to the interfacial adhesion
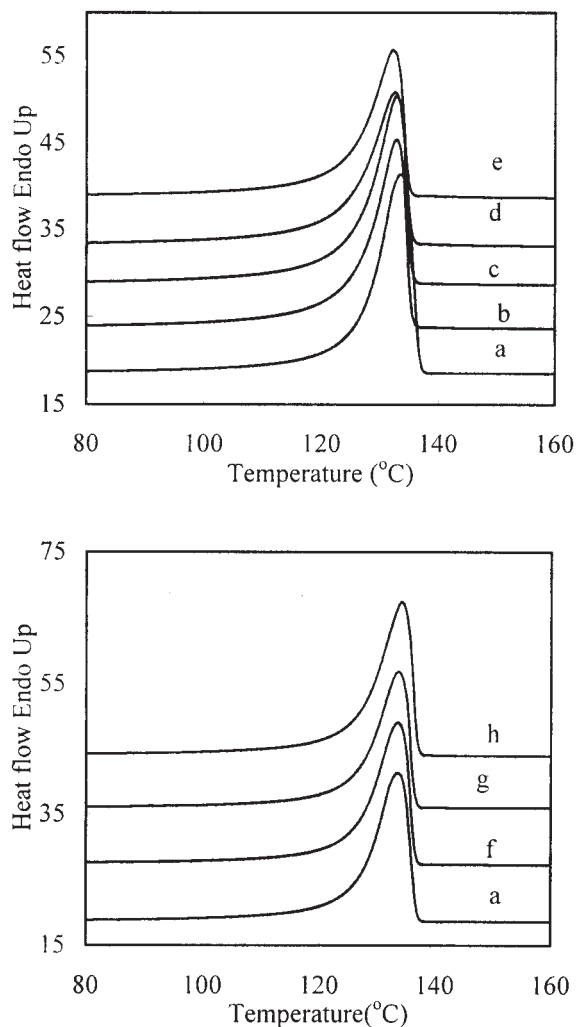
Figure 9 DSC curves of HDPE, HDPE-*g*-AA, and their composites with BT: (a) pure HDPE; (b) HDPE/DCP (0.2 phr); (c–e) HDPE/BT (2, 3, and 4 phr); (f–h) AA-modified HDPE/BT (2, 3, and 4 phr).

between the filler and the matrix. A strong interfacial adhesion leads to high tensile strength and a low elongation, whereas a weak interfacial adhesion leads to low strength and relatively high elongation.[16] For HDPE-*g*-AA/BT composites, BT was well exfoliated and there is strong interfacial adhesion between BT nanosheets and the polyethylene matrix, resulting in high strength and relatively low elongation. In HDPE/BT composites, however, BT is not intercalated and the interaction between BT aggregates and HDPE matrix is poor, resulting in poor tensile strength.

Thermal behavior of composites

Figure 9 and Table III display the melting temperature of polyethylene in HDPE-*g*-AA/BT and HDPE/BT composites, respectively. It is evident that the peak melting temperature and melting endotherms (Δ*H*) of HDPE-*g*-AA/BT composites were slightly lower than

that of HDPE-*g*-AA. When progressive addition of BT, the melting temperature and melting endotherms decreased slowly. These changes may be attributed to high interfacial adhesion between the HDPE-*g*-AA matrix and exfoliated clay, which reduces the mobility of crystallizable PE chain segments and subsequently reduces the crystallization ability.

In comparison, when we added 2, 3, and 4 phr BT to HDPE, we found that melting temperature and melting endotherms were nearly unchanged, inferring weak interaction between HDPE matrix and BT.

CONCLUSIONS

Chemical modification of both the polyolefin and bentonite clay is necessary to generate polyethylene/BT nanocomposites by melt compounding. XRD and TEM results indicated that AA promoted the dispersion and exfoliation of BT into HDPE. Most of the BT has exfoliated into single sheets in HDPE-*g*-AA/BT composites. While in HDPE/BT composites, most of the BT aggregates are not intercalated by PE chains. Consequently, with increasing BT content, the tensile strength and Young's modulus of HDPE-*g*-AA/BT nanocomposites increased, while that of HDPE/BT composites decreased. Moreover, the addition of BT to HDPE-*g*-AA decreased the melting temperature and the degree of crystallization of the matrix. In comparison, the addition of BT to HDPE did not affect the crystallization behavior of the latter.

References

1. Vaia, R. A.; Ishii, H.; Giannelis, E. P. Chem Mater 1993, 5, 1694.
2. Vaia, R. A.; Feukolsky, R. K.; Giannelis, E. P. Chem Mater 1994, 6, 1017.
3. Vaia, R. A.; Jandt, K. D.; Kramer, E. J.; Giannelis, E. P. Macromolecules 1995, 28, 8180.
4. Vaia, R. A.; Vasudevan, S.; Krawiec, W.; Scanlon, L. G.; Giannelis, E. P. Macromolecules 1995, 7, 154.
5. Kawasumi, M.; Hasegawa, N.; Kato, M.; Vshiki, A.; Okada, A. Macromolecules 1995, 30, 6333.
6. Kato, M.; Vsuki, A.; Okada, A. J Appl Polym Sci 1997, 66, 1781.
7. Hasegawa, N.; Kawasumi, M.; Kato, M.; Vsuki, A.; Okada, A. J Appl Polym Sci 1997, 67, 87.
8. Vsuki, A.; Kato, M.; Okada, A.; Kurauchi, T. J Appl Polym Sci 1997, 63, 137.
9. Dagani, R. Chem Eng News 1999, 77, 25.
10. Jeon, H. G.; Jung, H. T.; Lee, S. W.; Hudson, S. D. Polym Bull 1998, 41, 107.
11. Furuichi, N.; Kurokawa, Y.; Fujita, K.; Oya, A.; Yasuda, H.; Kiso, M. J Mater Sci 1996, 31, 4307.
12. Heinemann, J.; Keichert, P.; Thomann, R.; Mulhaupt, R. Macromol Rapid Commun 1999, 20, 423.
13. Gopakumar, T. G.; Lee, J. A.; Kontopoulou, M.; Parent, J. S. Polymer 2002, 43, 5483.
14. Wang, K. H.; Choi, M. H.; Koo, C. M.; Choi, Y. S.; Chung, I. J. Macromolecules 2002, 35, 5529.
15. Wang, K. H.; Choi, M. H.; Koo, C. M.; Choi, Y. S. Chung, I. J. Polymers 2001, 42, 9819.
16. Fang, Z.; Hu, Q. Angew Makromol Chem 1999, 265, 1.